


# Middle East Technical University

# Department of Electrical and Electronics Engineering

## EE463: Static Power Conversion I

## Final Report

Group Name: Battery Voltas

Student 1: Elif Topaloğlu - 2443984

Student 2: Erkin Atay Toka - 2443968

Student 3: Doruk Yazıcı - 2517225

Submission Date: 23.01.2024

# Table of Contents

# Introduction

The aim of this project is to design a Wind Turbine Battery Charger whose input power is supplied from a small wind turbine generator. The design should convert the varying AC voltage to DC voltage and current within the battery voltage and charge limitations. Battery and wind turbine specifications are available at the GitHub Repository.

In this report, the candidate AC to DC topologies for battery charging are discussed, and the analytical calculations and simulation results regarding the selected topology are displayed. Then, according to these results, the candidate components are chosen, the inductor is designed, and possible control techniques are found. Following the implementation of the project in real-life, tests are done on the circuit and the results are represented.

# Project Definition

An AC to DC type power converter circuit which will be operating as a battery charger unit should be designed. The input is a three-phase wind turbine supplying varying voltage and a constant current and voltage is expected from the output. The requirements of the project are given below:

- **Input Voltage:** $15V_{line-to-line}$ to $25V_{line-to-line}$
- **Battery Capacity:** $100Ah$
- **Battery Nominal Voltage:** $12V$
- **Output Current:** $10A$
- **Output Current Ripple:** $20\%$ of average current

# Topology Selection

In order to control the output current and voltage, a controlled rectifier topology or a diode rectifier with a buck converter topology must be selected. All the topologies that are considered are listed.

- **Three-phase thyristor rectifier:** This topology consists of one gate driver, six thyristors, and some passive elements. The average output of a three-phase thyristor rectifier is given below.

$$V_d = \frac{3\sqrt{2}V_{ll}}{\pi}\cos(\alpha)$$

  The firing angle is between 53.67 and 69.18 degrees to feed a 12 V battery when the input voltage range is $15V_{ll}$ to $25V_{ll}$. Although this topology is comparable with the three-phase diode rectifier with a buck converter, this topology is not chosen since it is more prone to errors at the controller part.
- **Three-phase diode rectifier with buck converter:** This topology consists of one gate driver, seven diodes, 1 MOSFET, and some passive elements. The average output of a three-phase diode rectifier with a buck converter is given below.

$$V_d = \frac{3\sqrt{2}V_{ll}}{\pi} D$$

The duty cycle is between 0.355 to 0.6 to feed a 12 V battery when the input voltage range is $15V_{ll}$ to $25V_{ll}$. These values are obtainable for buck converters. Moreover, compared to single-phase topologies, the input current THD is lowered due to the cancellation of 3rd harmonics, and the output voltage rippler magnitude and frequency decrease. This results in smaller passive components for filtering purposes. Also, compared to a phase thyristor rectifier, control of this topology is easier.

- **Three-phase diode rectifier with synchronous buck converter:** This topology is mainly the same as the three-phase diode rectifier with buck converter, but the free-wheeling diode at the buck converter is changed with a MOSFET with an inverted gate signal. At a traditional buck converter, the forward voltage of the free-wheeling diode increases the conduction losses, especially at high currents. Changing this diode to a low-resistance MOSFET at the synchronous buck will improve the converter's efficiency. Also, since this application is a low-voltage one, the output voltage can easily be affected by the diode on resistance. Thus, using a synchronous buck converter will be more logical. However, the complexity of the controller is increased due to the added inverted gate signal. Nevertheless, it is worth trying this topology due to the increased efficiency and low voltage drop on MOSFET.

The final decision of the team is designing a "Three-phase Diode Rectifier with Buck Converter" due to the easiness of control and implementation. The buck converter control will be closed loop so that the desired output current can be obtained. The controller implemented will be digital. Next, the analytical calculations and simulation results for the selected topology will be provided.

# Analytical Calculations

Considering the specifications of the project, analytical calculations are done for the ideal selected designs, which consist of a three-phase full-bridge diode rectifier and buck converter. Analytical calculations give a general understanding of the system and the values of the circuit elements, duty cycle, etc. After the ideal component values are calculated, further arrangements are made in the simulation to obtain a better working system. In order not to set the simulation values far from being reasonable and by just arranging the values by trial and error, having an insight into the component values is valuable, which necessitates the analytical calculation part. Analytical calculations done before the simulation are presented below.

First, the average output of the three-phase full-bridge diode rectifier is calculated as it is the input of the buck converter and determines the required duty cycle values for the project. Using the formula below, maximum, and minimum input voltage values for the buck converter are calculated.

$$V_{out,average} = \frac{3\sqrt{2}}{\pi} \cdot V_{line-to-line}$$

$$V_{in,min} = \frac{3\sqrt{2}}{\pi} \cdot 15 \cong 20.3\, V$$

$$V_{in,max} = \frac{3\sqrt{2}}{\pi} \cdot 25 \cong 33.8\, V$$

If the nominal output battery voltage is known, using the input voltages of the buck converter and the output nominal voltage, the maximum and minimum duty cycles required for the project can be calculated.

$$D_{max} = \frac{V_{out}}{V_{in,min}} = \frac{12}{20.3} \cong 0.59$$
$$D_{min} = \frac{V_{out}}{V_{in,max}} = \frac{12}{33.8} \cong 0.36$$

One of the most essential elements of the buck converter is the inductor. The inductance value should be calculated to have the buck converter functioning appropriately. There are two operating modes of a buck converter: continuous conduction and discontinuous conduction. In the continuous conduction mode, the inductor current is always positive, and for the discontinuous conduction mode, the current is positive for some time and zero otherwise. The point where the minimum inductor current equals zero is defined as the critical conduction mode. The inductance value calculated for this mode is called the required inductance, and if one wants to operate in the continuous conduction mode, the selected inductance should be larger than the critical inductance value. The calculation of the critical inductance is given below.

$$L_{critical} = \frac{(1 - D_{\max}) \cdot V_{max}}{2 \cdot f_s \cdot I_{out} \cdot (1 - I_{ripple})}$$

$$L_{critical} = \frac{(1 - 0.59) \cdot 12}{2 \cdot 50 \cdot 10^3 \cdot 10 \cdot 0.8} \cong 6.15\ \mu H$$

For this calculation, the switching frequency is used and selected as 50 kHz. The reason for this selection can be understood by examining the effects of switching frequency. If the switching frequency increases, the output current ripple decreases, which is desired for this system. Due to this reason, a low switching frequency cannot be selected as it is not possible to meet the maximum 20% current ripple criterion. With low frequency, this criterion can be met by increasing the inductance value; however, increasing it makes the inductor bigger and more expensive. Therefore, a neat design for low switching frequency selection cannot be achieved. Moreover, increasing the frequency is not desired as it increases the loss due to switching. Therefore, a 50 kHz switching frequency is selected as it is reasonable and adequate regarding the requirements and efficiency concerns.

Finally, the capacitor for input and output of the buck converter should be determined. Formulas to calculate these capacitor values are presented below.

$$C_{out} = \frac{(1 - D_{\min}) * D_{\min} * I_{out,max}}{f_s * \Delta V_{in}}$$

$$C_{out} = \frac{(1 - 0.36) * 0.36 * 10 * 1.2}{50 * 10^3 * (33.8 - 20.3)} \cong 4.1\ \mu F$$

$$C_{in} = \frac{1 - D_{\min}}{8 * L_{critical} * f_s^2}$$

$$C_{in} = \frac{1 - 0.36}{8 * 6.15 * 10^{-6} * (50 * 10^3)^2} \cong 5.2\ \mu F$$

These are the minimum values for the capacitors. In a real-life application, capacitors are mainly selected to decrease the ripples on current and voltage waveforms so that in the component selection, the ripple minimization will be the mainly considered design problem.

These calculations are done under the assumption of 100% efficiency, which cannot be achieved in real-world design using lossy elements. However, analytical calculations are still necessary to have valuable insight into the element values so that further selection can be improved using the simulation tools easily without blindly following the trial-and-error method. All the calculations in this part are done using documents that are presented in the reference part of the report. [1] [2] In the following section, simulation results for the design will be presented.

# General Solution and Overall Design

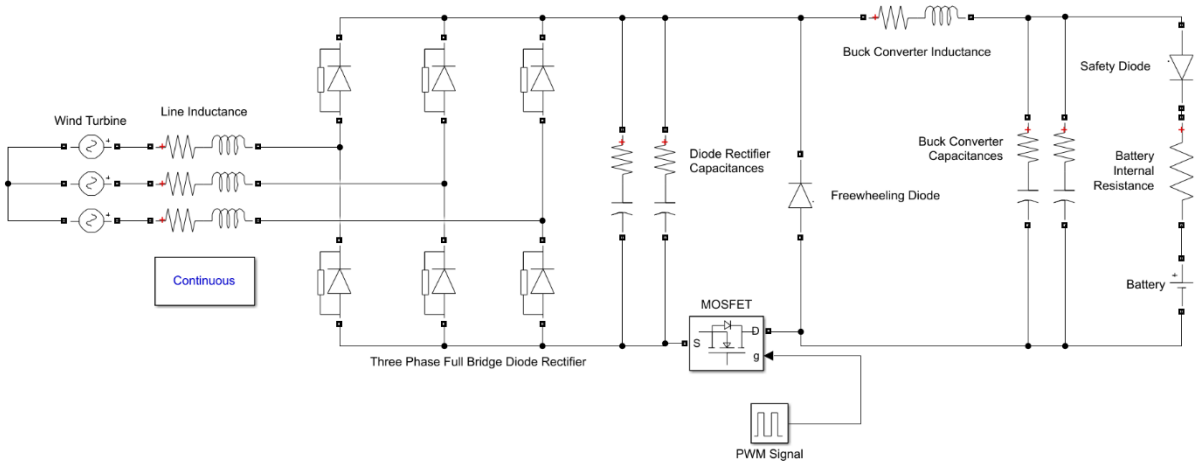


**Figure 1. Circuit Schematic of the Wind Turbine Battery Charger**

Figure 1. represents the design of the circuit that is proposed for the Wind Turbine Battery Charger. One can easily notice that compared with a classical buck converter, the given circuit has its MOSFET -switching component- placed at the so called “low-side” of the circuit. With a given configuration, the “source” leg of the MOSFET is connected to a node with a lower voltage compared to the “high side” placement. As the source voltage is lower, the gate voltage that should be applied to outrun the gate-source threshold voltage -$V_{GS(th)}$- also decreases, which makes it easier to operate the MOSFET.

For the three-phase rectification, a “Three-Phase Full Bridge Diode Rectifier” circuit is built using 6 of the DSS16-01A Schottky diodes. The main reason for not using a rectifier module but making with hand is that the opening voltages of the diodes used in a rectifier module is way higher than the diodes that are used in the project so that overall losses are decreased, and efficiency is increased. To the output of the rectifier, 2 of the $1000\mu F$ capacitors are connected in parallel to neglect the ripples on voltage and current, so that we can have a near DC voltage at the input of the buck converter.

A critical point is that the “reference node” of the circuit is set as the node to which the source leg of the MOSFET is connected. It can be thought of as the node that the ground connections are done.

It was stated that the controller of the circuit is chosen as a digital one, so that the team decided to use an “Arduino UNO” to assume the mantle. The main reasons to choose Arduino UNO as a digital controller are, easiness of operation and updatability, existence of digital output pins, existence of analogue input pins, low power consumption, and compatibleness with many modules in the market. Using the Arduino UNO and a current sensor -ACS712-, the output current value will be read, processed in the control method implemented, and the resulting PWM signal will be applied from a digital output pin to operate the MOSFET.

The switching component used is an IRF540N 100V 33A N-Channel Power MOSFET. As the MOSFET has high current and voltage ratings, the PWM signal being sent from the Arduino UNO to the gate of MOSFET is not sufficient to operate it. To overcome this issue, IR2106 High and Low Side Gate Driver is used. A gate driver basically amplifies the signal that is being sent to it so that the current applied to the gate of a MOSFET increases, which opens it up.

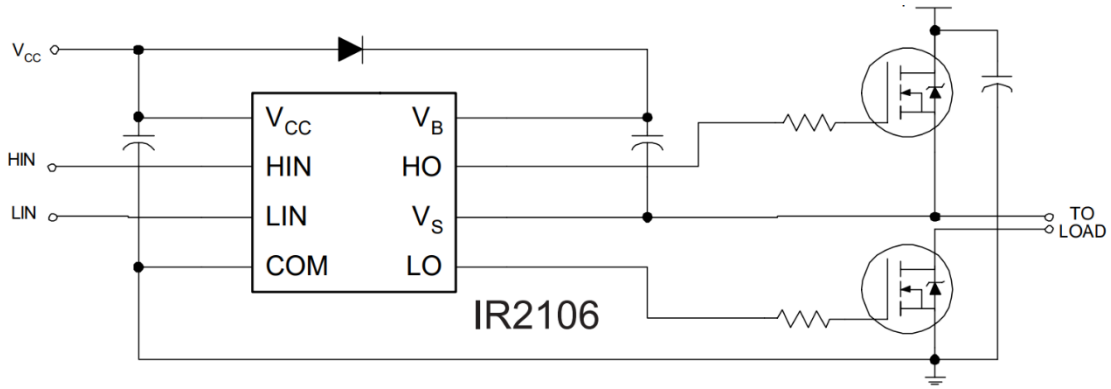


**Figure 2. IR2106 Connections**

Figure 2 shows a typical connection made with IR2106. As mentioned before, the MOSFET is placed to the low side of the buck converter so that pin “LIN” will be used to obtain the PWM signal from Arduino UNO and pin “LO” will be used as an output to the gate of the MOSFET. The input capacitance between $V_{CC}$ and “COM” pin is chosen as $100\mu F$, and the resistance between the pin “LO” and gate of the MOSFET is chosen as $4.22\Omega$. IR2106 can work with voltages up to $25V$ so that it is powered from the “LM2596 DC-DC Step Down Converter”.

LM2596 DC-DC Step Down Converter is basically a buck converter module that is used to regulate the high DC voltage at the output of the three-phase rectifier to a level that the Arduino UNO, IR2106, and the cooling fans can use. It can regulate an input voltage between $4V_{DC} - 35V_{DC}$ to a range of $1V_{DC} - 30V_{DC}$. As the maximum operating voltage of the fans and the Arduino UNO is 12V, the converter is set to supply 11V for safety, which is enough to power up all of the devices.

**Figure 3. LM2596 DC-DC Step-Down Converter**

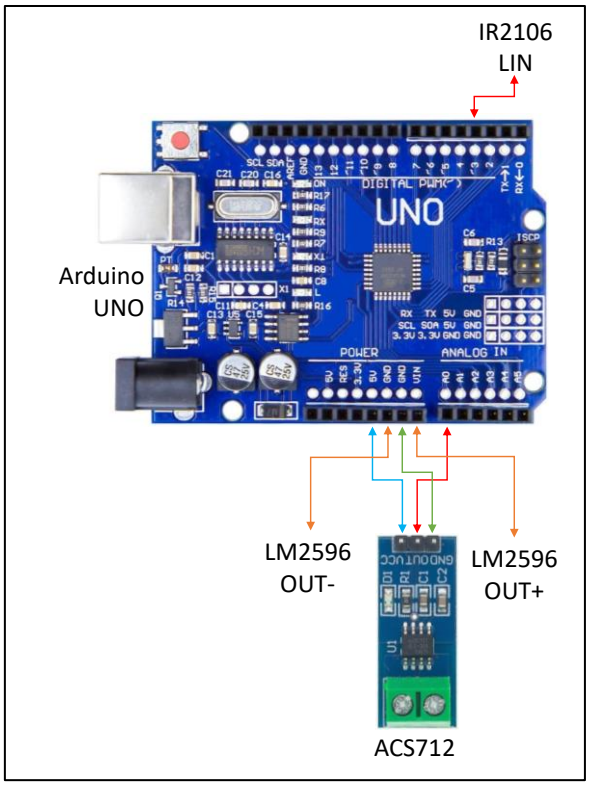


**Figure 4. Arduino UNO Connections**

Figure 4 shows the connections made on the Arduino UNO board. A0 pin is used for the analog input coming from the ACS712 current sensor, "Pin 3" is used as an output which sends the PWM signal to the "LIN" pin of the IR2106 gate driver. The ACS712 is powered by the 5V pin, and the Arduino UNO itself is powered by the LM2596. The inductor used in the buck converter is chosen as $120\mu H$ to minimize the output current ripple, and decrease the size of the core needed, which is advantageous for the size of the overall circuit. 2 of the $470\mu F$ capacitors are used in the output of the buck converter. The freewheeling diode and the safety diode are chosen as the same diode, which is a DSS30I100PA Schottky diode. If a safety diode is not used at the output, the battery can burn the circuit by supplying high current. The safety diode prevents this, as a current cannot flow from cathode to the anode of the diode. Another critical point is that is the output current is $10A$, the forward voltage of the selected diode should be small so that the conduction losses on the diode can be minimized and efficiency can be enhanced.

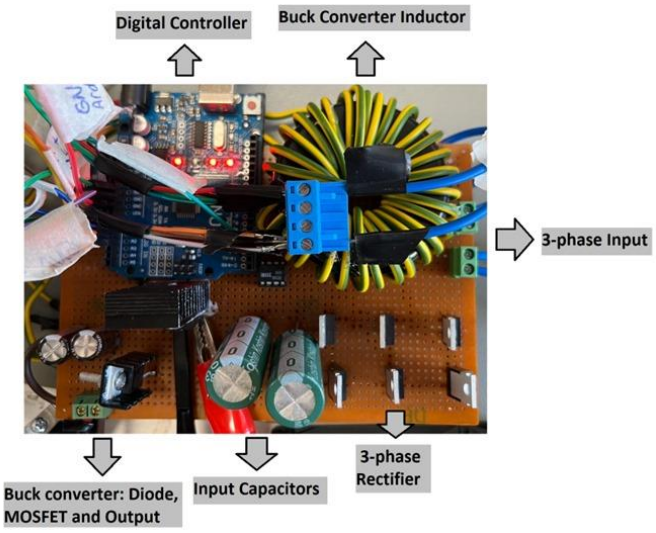


**Figure 5. Implemented Circuit**

# Simulation Results

A simulation was conducted to confirm the functionality of a three-phase full-bridge diode rectifier coupled with a conventional buck converter model. The complete simulation model is outlined below, omitting measurement units for simplicity.

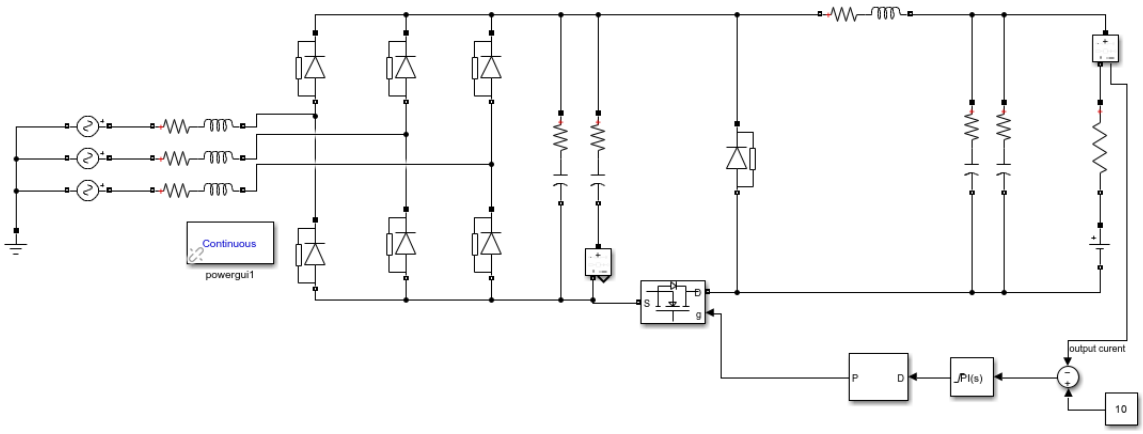


**Figure 6. Simulation of the Final Design**

In the Simulink simulation, a resistor, and a DC voltage source in series with the resistor are utilized to imitate the battery at the output.[3] The selection of the series resistance value is based on research into a battery with a similar capacity and voltage.[4]

To achieve more precise and comparable outcomes with the real-world scenario, components are presented with their imperfections, particularly the series resistances. Additionally, the simulations consider the commutation effect due to source inductance. Snubber values are also computed and included in the simulation for both the diodes and the MOSFETs to limit sudden changes of the current and the voltage.

Moreover, the simulation incorporates two parallel branches for both input and output capacitors. The reason of several parallel capacitors is intended to decrease the impact of capacitor series resistance (ESR). ESR worsens output ripple; hence, by connecting multiple capacitors in parallel, the aim is to reduce ESR effects.

The simulation results for this topology are displayed below, confirming the proper functionality of the design. The outcomes confirm that the design meets voltage requirements and current ripple constraints, maintaining an approximately 10% ripple.

Simulation results for this topology are presented below for rectifier, battery, MOSFET and the inductor.

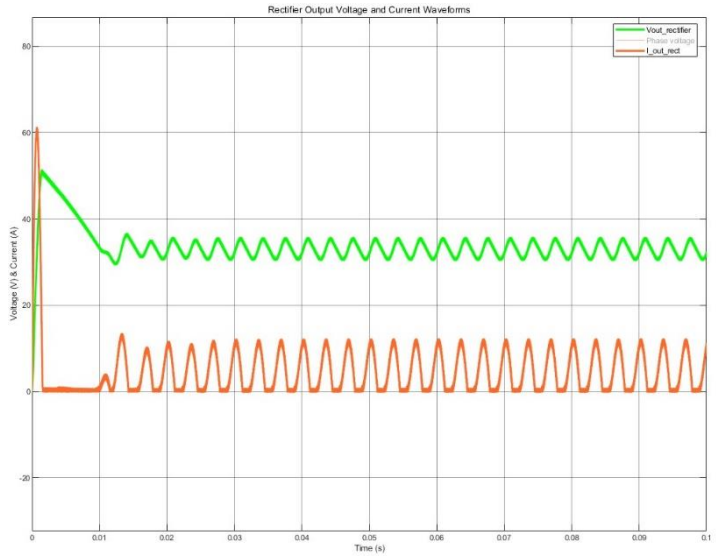


**Figure 7. Rectifier Voltage and Current Waveforms**

As can be seen from the figure above, voltage at the output of the rectifier part is close to DC voltage with reasonably small voltage ripple. The current has more ripples than the voltage; however, by selecting the diodes and capacitors to withstand this current ripple, this did not become a problem. The waveforms for the MOSFET and inductor wis presented below.

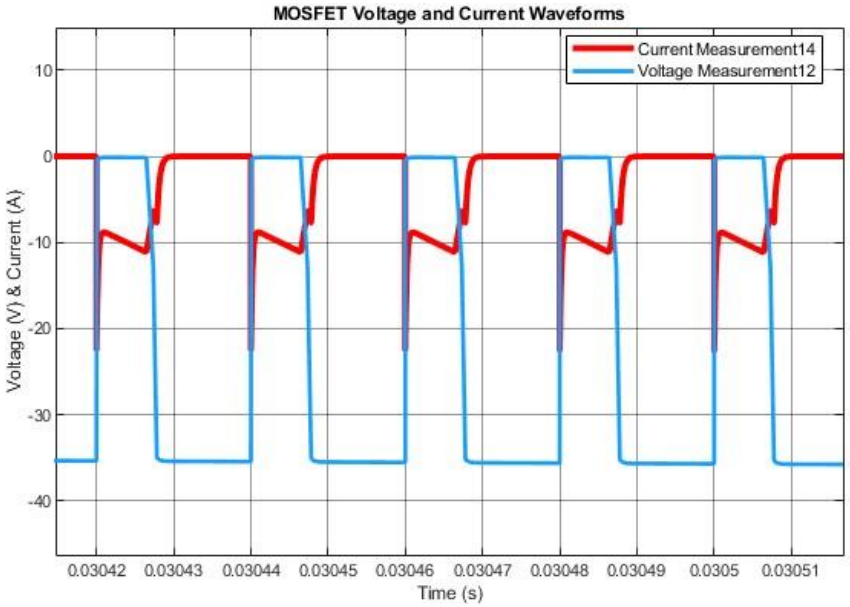


**Figure 8. MOSFET Voltage and Current Waveforms**

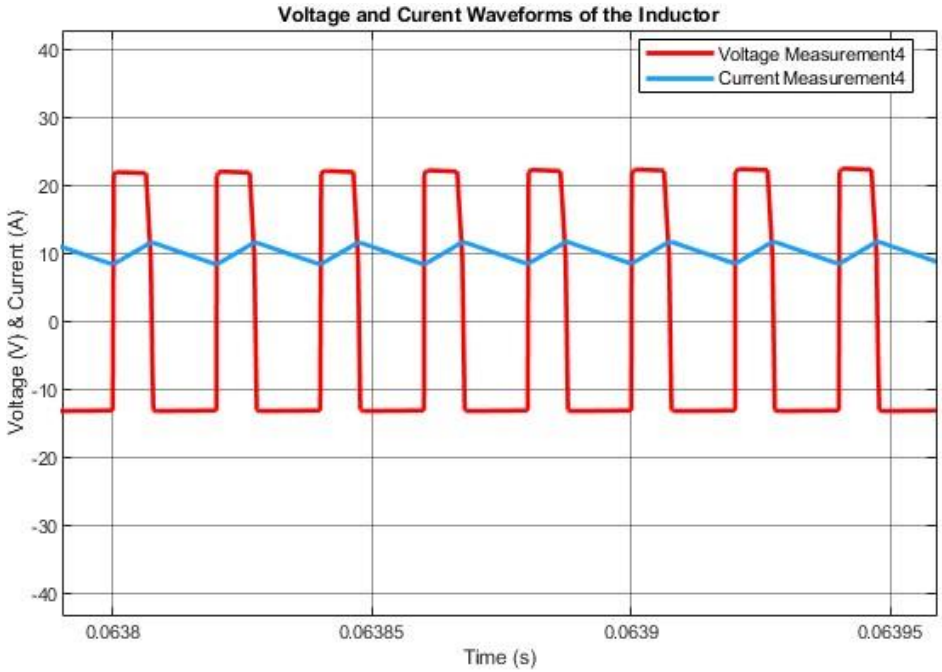


**Figure 9. Inductor Current and Voltage Waveforms**

As can be seen from the plots, current and voltage waveforms fit the analytical expectations since the current flowing through the inductor increases when the buck is on state and the MOSFET is off. For the off state, inductor current decreases as it can also be verified from the inductor voltage becoming negative and the MOSFET starts to conduct the current flowing through the circuit. Even though the simulation results fit the analytical patterns, the waveforms are not directly the same and have some nonidealities. This is expected as the simulation includes nonidealities that will be faced during the real design. Also, one of the important conclusions that should be made is that the more similar the simulation is to the real circuit, the closer the simulation data is to the data obtained in real life. The MOSFET current and voltage waveforms are surprisingly similar to real-world data.

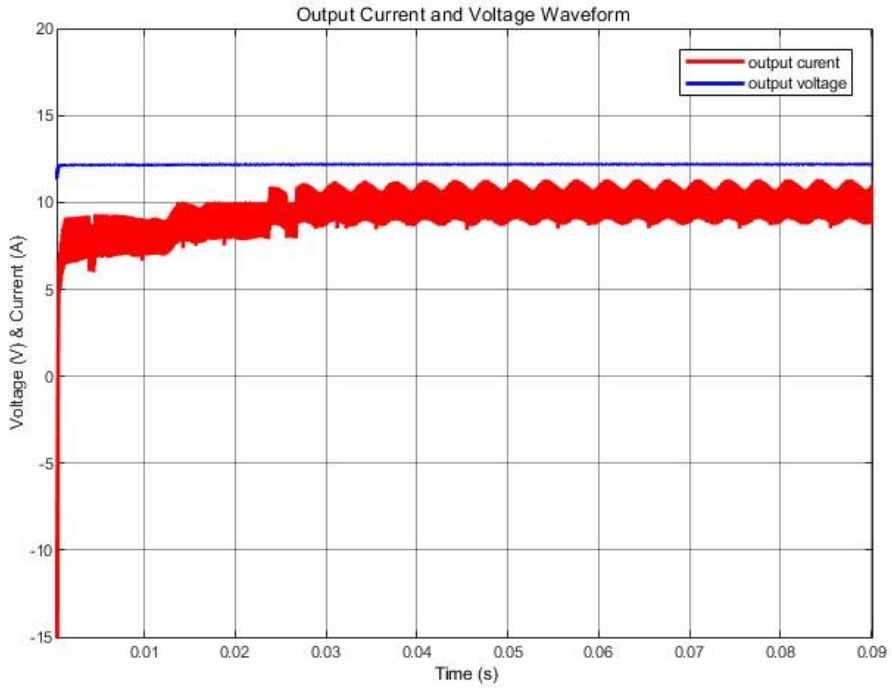


**Figure 10. Battery Voltage and Current Waveforms**

Finally, the output voltage and the current waveforms are presented above. As it can be seen from the figure, the design is able to charge the battery with meeting the current ripple constraints. In the following part of the report, appropriate components will be selected for the overall design. Before the selection, all the current and voltage waveforms for the components are measured, and using a safety factor, maximum voltages and currents on the components are determined for selection.

# Component Selection

Following the completion of the simulations, component selections are made. An important point is that a 40% safety margin is set in all of the components that are used to protect the circuit, prevent overdesign, and decrease the power losses. Datasheets of the components can be found in the GitHub Repository of the project. Components are provided from the companies located in Turkey such as "Özdisan" and "direnç.net".

- **IRF540N**

MOSFET used in the buck converter is the IRF540N from International Rectifier. The considered ratings of the MOSFET are given in Table 1.

**Table 1. IRF540 MOSFET Ratings**

| **Parameter** | **Value** | **Unit** |
|---|---|---|
| Continuous Drain Current $I_D$ @ $T_C = 25°C$ | 33 | A |
| Continuous Drain Current $I_D$ @ $T_C = 100°C$ | 23 | A |
| Drain-to-Source Breakdown Voltage $V_{(BR)DSS}$ | 100 | V |
| Gate Threshold Value $V_{GS(th)}$ | 4 | V |
| Static Drain-to-Source on Resistance $R_{DS(on)}$ | 44 | mΩ |

In the simulations, the maximum current observed is approximately 22A, and the maximum voltage observed is approximately 45V, which appears to be at the start-up, and it drops to 29V in steady-state operation. It is contained in a TO-220 package. The MOSFET chosen fits the requirements of the system.

- **IR2106**

Arduino UNO, which is the digital controller of the circuit, is not capable of driving the MOSFET through its pins as the maximum current it can supply is not enough to supply the enough gate charge. To be able to operate the MOSFET, IR2106 Gate Driver is used. It is a high and low side gate driver from the International Rectifier.

- **DSS16-01A**

In the three-phase rectifier part of the circuit, 6 of the DSS16-01A Power Schottky diodes from IXYS are used. It is contained in a TO-220 package. The considered ratings of the diode are given in Table 2.

**Table 2. Rectifier Diode Ratings**

| **Parameter** | **Value** | **Unit** |
|---|---|---|
| Average Forward Current $I_{FAV}$ | 16 | A |
| Average Forward Voltage $V_{FAV}$ | 0.64 | V |
| Maximum Repetitive Reverse Voltage $V_{RRM}$ | 100 | V |

Even though the input voltage varies between $15V_{RMS}$ and $25V_{RMS}$, the voltages and currents measured on the diode stay in the limits.

- **DSA30I100PA**

As the free-wheeling diode of the buck converter, and the safety diode placed in front of the battery, DSA30I100PA Schottky diodes from IXYS are used. It is contained in a TO-220 package. The considered ratings of the diode are given in table 3.

**Table 3. Buck Converter & Safety Diode Parameters**

| Parameter | Value | Unit |
|---|---|---|
| Average Forward Current $I_{FAV}$ | 30 | A |
| Average Forward Voltage $V_{FAV}$ | 0.78 | V |
| Maximum Repetitive Reverse Voltage $V_{RRM}$ | 100 | V |

- **WL1V477M10020PA**

In the output of the buck converter, 2 of the $470uF\ 35V$ capacitors from SAMWHA are placed to handle the voltage and the current ripples at the output side. The equivalent series resistance of the capacitor is given as $0.054\Omega$, and the ripple current is given as $1.1A_{RMS}$.

- **PKLH-063V102MJ355**

In the output of the three-phase rectifier, 2 of the $1000uF\ 63V$ capacitors from KOSHIN are placed to handle the voltage and the current ripples at the input side. The equivalent series resistance of the capacitor is given as $0.05\Omega$, and the ripple current is given as $2.45A_{RMS}$. As the ripples in the input side are high, a capacitor with a high capacitance is chosen.

- **Buck Converter Inductor**

The inductor of the buck converter is designed, implemented, tested, and verified by the team. The inductance is set to $120\mu H$. The core used is 0079192A Kool M$\mu$.

- **ACS712ELC-30A**

The output current measurement is done via the ACS712ELC-30A current sensor. It is capable of measuring currents in range of $\pm 30A$. It works with 5V that is supplied from Arduino UNO and it sends the measurement data in a digital manner.

- **LM2596 DC-DC Step Down Converter**

To supply the Arduino UNO, IR21106, and cooling fans, an LM2596 buck converter is used. It is supplied from the output of the three-phase rectifier.

- **Arduino UNO**

The controller of the circuit is chosen to be digital so that an Arduino UNO is used. It gathers the output current data from the ACS712 current sensor and controls the duty cycle of the PWM signal that is sent to the IR2106 gate driver.

- **Fan**

A 12V 92x92x25mm 3000rpm fan is used to cool down circuit components via forced convection.

## Inductor Design

The determined inductance of the buck converter is 120 µH, so that both CCM operation and ripple condition is met. In this part magnetic design of the inductor and core selection will be explained.

First the cable that will be used to wind the core is selected. The average current of a buck converter inductor is the output current. Since the battery will be charged with 10A the inductor current will also be 10 A. Thus, high voltage cables that can endure more than 10A are investigated. H07V-K1.5 which can carry

up to 16 A is selected. The copper area of the cable is 1.5 mm$^2$. Also, the average outer diameter of the cable with insulation is 2.9 mm. The area of this cable can be calculated from:

$$A_{cable} = \pi \left(\frac{D}{2}\right)^2 = 6.6\, mm^2$$

Then permeability vs DC bias curves of the Kool $M_\mu$ cores that are available in the laboratory are obtained from Magnetics [5] The permeability fit formulas from [5] are given in Figure 11 and the permeability vs DC magnetizing field (Oe) is given in Figure 12.

Fit Formula

% initial permeability = $\frac{1}{(a + bH^c)}$ where H is Oersteds (Oe)

| | Perm | a | b | c |
|---|---|---|---|---|
| Kool Mμ® Toroids | 14μ | 0.01 | 4.938E-08 | 2.000 |
| | 26μ | 0.01 | 5.226E-07 | 1.819 |
| | 40μ | 0.01 | 2.177E-06 | 1.704 |
| | 60μ | 0.01 | 2.142E-06 | 1.855 |
| | 75μ | 0.01 | 3.885E-06 | 1.819 |
| | 90μ | 0.01 | 5.830E-06 | 1.819 |

**Figure 11. KoolMu Toroid Permeability Fit Formula**

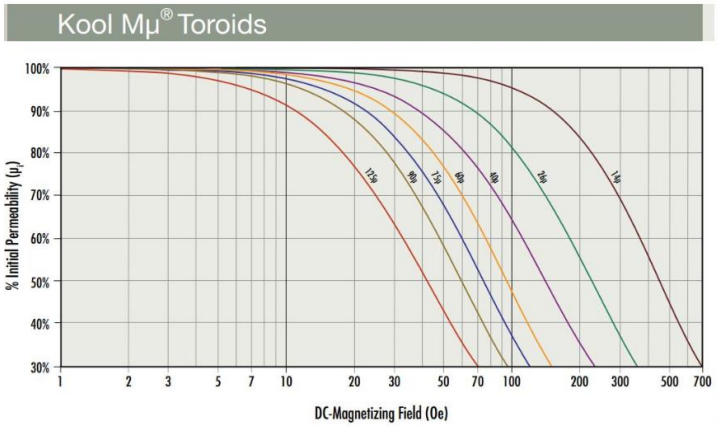


**Figure 12. Permeability vs DC Magnetizing Field Curve**

From this fit formula and physical properties of the magnetic core $A_L$, which is inverse of the reluctance, is written as a function of the MMF which is turns number times the current. MMF and $A_L$ can be written in terms of relative permeability and magnetizing field as follows:

$$A_L = \frac{1}{R} = \frac{\mu_0 \mu_r A}{l}$$

$$MMF = NI = H\, l$$

$$l = magnetic\ path\ length$$

$$A = cross\ sectional\ area\ of\ the\ core$$

$$A_L = \frac{\mu_0\, \mu_r\, A\, l}{100\left[a + b\left(\frac{MMF}{l\,\frac{Oestred}{A/m}}\right)^c\right]}$$

Since the inductor current is known which is 10 A the inductance can be computed from these parameters.

$$L = \frac{N^2}{R} = \frac{MMF\ A_L}{I^2}$$

The fixed-point iteration method is applied to find the turns number (N) that will yield 120 µH inductance. The block diagram of the algorithm is given in Figure 13.

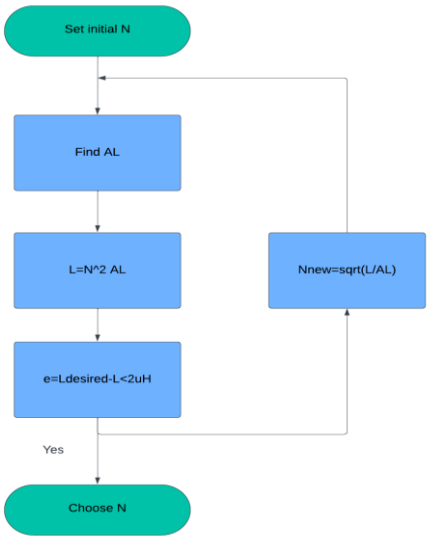


**Figure 13. Fixed Point Iteration Block Diagram**

According to the selected turns number and the window area of the core $A_{window}$ the fill factor is calculated as follows.

$$Fill\ Factor = \frac{N\ A_{cable}}{A_{window}}$$

More than 60% fill factor is not plausible. To be safe it is aimed that the fill factor will be kept lower than 50%.

According to these considerations 0079192A7 Kool Mµ core is selected. The typical DC Bias curve is given in Figure 4. The turns number is determined as 32 which gives $A_L$ 121.8 nH/T$^2$.

$$L = N^2 A_L = 124\ \mu\text{H}$$

The window area of the selected core is 514 mm$^2$. Fill factor can be calculated as follows.

$$Fill\ Factor = \frac{NA_{cable}}{A_{window}} = 0.411 = 41.1\%$$

As it can be seen that the fill factor is smaller than %50 hence it is possible to design this inductor. According to the datasheet, the winding length per turn for 40% fill factor is 77.8 mm. Hence, the total length of the cable must be approximately 2.5m. The resistance of the selected cable is 13.3 mΩ/m. The expected resistance of the cable is 33.25 mΩ.

The measured resistance and the inductance from the LCR meter at switching frequency 50kHz, are $111m\Omega$ and $142mH$ respectively. Since the LCR meter applies a small voltage, the calculated inductance is without the saturation. Hence the expected result is given below.

$$L_{unsaturated} = N^2 A_{L,max} = 141.36\ mH$$

It can be seen that measured inductance is very close to the calculated result. For saturation, a special test is applied to the inductor which will be explained in Test Results section.

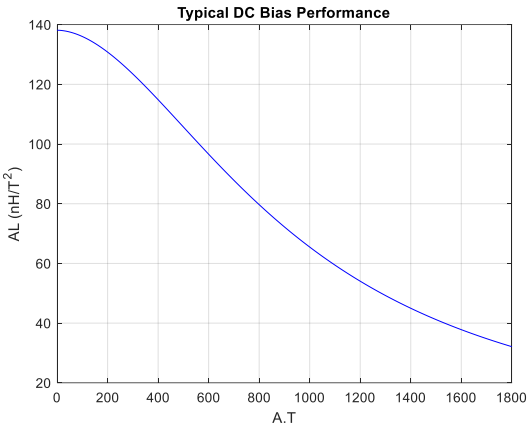


**Figure 14. Typical DC Bias Curve of 0079192A7**

# Test Results

In this section, the tests that are conducted up to demo day are explained and results are shared. Two tests are conducted to investigate the inductor design. Then, the overall circuit is tested with R load. At last, the circuit is tested with battery supplying 10A.

## Inductor Tests

Two tests are conducted for the design of the inductor. In the first one, the inductance of the inductor is tested with 10A DC bias and effect of the saturation will be observed. In the second test the heating of the inductor is observed with 10 A DC.

- **Inductance Test**

In this test the inductance is observed when 10A is passing through the core. In other words, the effect of the saturation on the inductance will be observed. It is aimed that the inductance will be close to $120\mu H$. In order to test the inductance, the following setup given in Figure 15 is constructed.

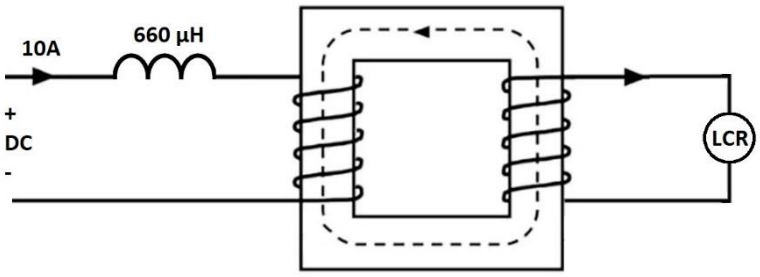


**Figure 15. Inductance Test Setup**

Two windings are wound to the inductor. The one on the left carries the DC 10A current which will saturate the core. For this winding the H07V-K with $1.5mm^2$ copper area is used. The second winding is used to measure the inductance with LCR meter. This circuit acts as a transformer; hence the inductance of the core can be calculated under 10 A DC bias. Since LCR meter applies a small voltage to measure inductance, a thinner cable can be used. In this case AWG15 is used. The equivalent circuit which is seen by the LCR meter of this setup is provided in Figure 16.

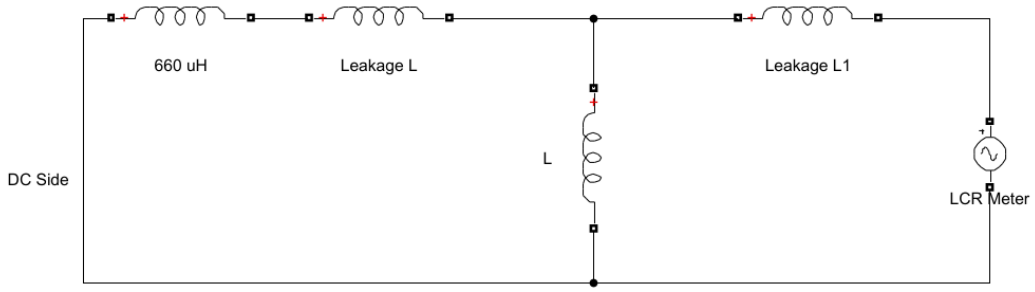


**Figure 16. Equivalent Circuit seen by the LCR Meter**

Since the switching frequency is 50 kHz the LCR meter is arranged to apply 50 kHz 1 $V_{PP}$ voltage. Since there are large capacitors inside the DC supply from LCR meters point of view that part is shorted. Thus, if 660 µH is not used at the input side the value that is read by the LCR meter will be as follows.

$$L_{LCR} = L_{leakage} + (L // L_{leakage})$$

Since leakage inductance is much smaller than the wound inductance the measured inductance will be approximately $2L_{leakage}$. Thus, a higher inductor, which is 660 µH, is connected to the DC side so that the measured inductance will be as follows.

$$L_{LCR} = L_{leakage} + \left[L // \left(L_{leakage} + 660\ \mu\text{H}\right)\right] \cong L_{leakage} + [L // (660\ \mu\text{H})] \cong L // (660\ \mu\text{H})$$

The inductance is measured as 106 µH by the LCR meter. This will yield $L = 126.3\ \mu\text{H}$ which shows the inductor design is successful.

- **Inductor Heating Test**


**Figure 17. DC Supply Readings**

It can be seen that the total copper loss is 11.7 Watt.

The core losses of the inductor is calculated from the Magnetics [5]. The following procedure is applied to find core losses of 0079192A7.

$$H_{max} = \frac{N}{l}\left(I + \frac{\Delta I}{2}\right) = \frac{32}{125\ 10^{-3}}\left(10 + \frac{2}{2}\right) = 2816\frac{A}{m} = 35.387\ Oe$$

$$H_{min} = \frac{N}{l}\left(I - \frac{\Delta I}{2}\right) = \frac{32}{125\ 10^{-3}}\left(10 - \frac{2}{2}\right) = 2304\frac{A}{m} = 28.953\ Oe$$

The maximum and minimum flux density is calculated from the below relation [5].

DC Magnetization Curves

Fit Formula

$B = \left[\frac{a + bH + cH^2}{1 + dH + eH^2}\right]^x$ where B = Tesla (T), H = Oersteds (Oe)

| | Perm | a | b | c | d | e | x |
|---|---|---|---|---|---|---|---|
| Kool Mμ® Toroids | 14μ | 3.918E-02 | 1.856E-02 | 4.812E-04 | 1.390E-01 | 4.478E-04 | 1.875 |
| | 26μ | 3.763E-02 | 1.712E-02 | 5.155E-04 | 9.190E-02 | 4.909E-04 | 1.812 |
| | 40μ | 3.789E-02 | 1.632E-02 | 5.355E-04 | 7.365E-02 | 5.110E-04 | 1.665 |
| | 60μ | 3.601E-02 | 1.721E-02 | 5.401E-04 | 5.624E-02 | 5.156E-04 | 1.577 |
| | 75μ | 3.111E-02 | 2.286E-02 | 5.343E-04 | 5.568E-02 | 4.982E-04 | 1.614 |
| | 90μ | 2.965E-02 | 2.538E-02 | 5.142E-04 | 5.305E-02 | 4.867E-04 | 1.578 |
| | 125μ | 2.730E-02 | 2.946E-02 | 5.038E-04 | 5.274E-02 | 4.639E-04 | 1.471 |
| Kool Mμ® E Cores, U Cores & Blocks | 14μ | 5.216E-02 | 1.507E-02 | 4.323E-04 | 1.036E-01 | 5.174E-04 | 1.952 |
| | 26μ | 2.710E-02 | 9.151E-03 | 4.036E-04 | 7.636E-02 | 3.986E-04 | 1.515 |
| | 40μ | 4.990E-02 | 1.537E-02 | 5.792E-04 | 7.263E-02 | 5.542E-04 | 1.689 |
| | 60μ | 4.286E-02 | 1.787E-02 | 6.044E-04 | 6.335E-02 | 5.529E-04 | 1.586 |
| | 90μ | 3.157E-02 | 2.186E-02 | 6.059E-04 | 5.720E-02 | 5.696E-04 | 1.476 |
| Kool Mμ® EQ Cores | 26μ | 4.488E-02 | 1.747E-02 | 5.106E-04 | 9.447E-02 | 4.342E-04 | 1.822 |
| | 40μ | 4.831E-02 | 1.637E-02 | 5.832E-04 | 7.751E-02 | 5.059E-04 | 1.692 |
| | 60μ | 4.286E-02 | 1.787E-02 | 6.044E-04 | 6.335E-02 | 5.529E-04 | 1.587 |

Kool Mμ® Toroids

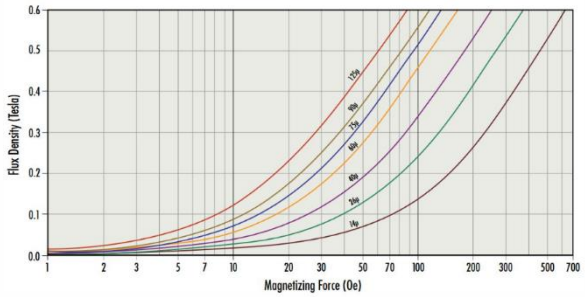


**Figure 18. DC Magnetization Curves of KoolMu Cores**

From the relation given in Figure 18; maximum, minimum, and ripple of the flux density is calculated as follows:

$$B_{max} = 0.2027\ T$$

$$B_{min} = 0.1679\ T$$

$$B_{pk} = \frac{B_{max} - B_{min}}{2} = 0.0174\ T$$

The core losses can be again calculated from the core loss density fit function given by [5].

$$P_L = 9.416\ mW/cm^3$$

$$P_{core} = P_L\ A\ l = 0.2695\ W$$

It can be seen that the core losses are very small compared to the copper losses, hence; their effect on the temperature rise is negligible.

Core Loss Density Curves

Fit Formula

$P = aB^bf^c$ where B = Tesla (T), f = kilohertz (kHz)

| | Perm | a | b | c |
|---|---|---|---|---|
| Kool Mμ® Toroids | 14μ | 80.55 | 1.988 | 1.541 |
| | 26μ, 40μ | 52.36 | 1.988 | 1.541 |
| | 60μ, 75μ, 90μ, 125μ | 44.30 | 1.988 | 1.541 |

**Figure 19. Core Loss Density Fit**

The inductor is heated for 80 minutes in $25\ °C$ environment and its temperature are measured with a thermal camera. The data is tabulated in Table 4 and plotted in Figure 20.

**Table 4. Inductor Temperatures**

| $\Delta t$ (min) | $\Delta T$ (°C) |
|---|---|
| 0 | 25.6 |
| 3 | 33.7 |
| 5 | 35.8 |
| 10 | 39.2 |
| 15 | 42.4 |
| 20 | 44.1 |
| 30 | 46.6 |
| 45 | 49.1 |
| 65 | 51.2 |
| 80 | 51.2 |

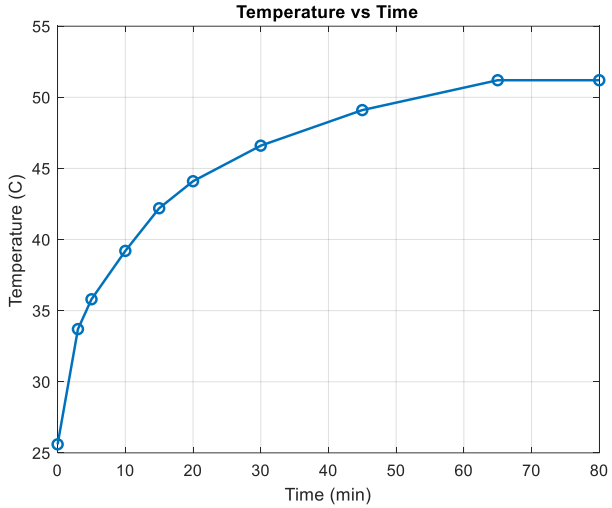


**Figure 20. Inductor Temperature (C) vs. Time (min)**

From Figure 20, it can be seen that the temperature of the core is settled at $51.2\,°C$ after 65 minutes. Also, after 5 minutes, which is the expected duration of the battery charging the inductor temperature reached $35.8\,°C$ which is quite safe.

## Resistive Load Test

Before testing the circuit with battery, it is tested with resistive load. The tested circuit is given in Figure 21.

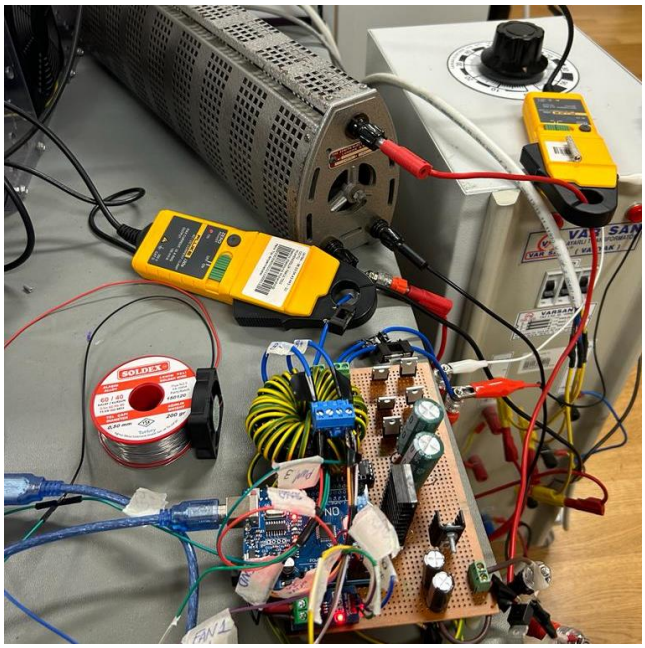

**Figure 21. Circuit Connection with Rheostat**

First, the controller is adjusted to set the output current to 5A before trying with 10A. The rheostat is set to 3 Ω. The circuit connected to rheostat and oscilloscope readings are given in Figure 22 and Figure 23 respectively.

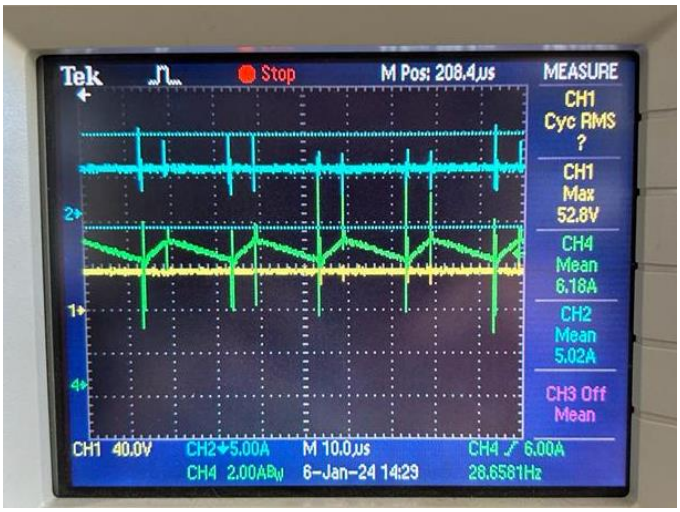


**Figure 22. Oscilloscope Results for Resistive Load with 5A**

In Figure 22 CH1 and CH3 are the output and inductor currents respectively. It can be seen that the controller managed to keep the mean output current at 5.02 A as expected. Also, the current ripple is quite small.

After that the circuit is tested with 0.5 Ω and the output current is set to 10A. Results are given in Figure 23. CH1, CH2 and CH4 measure input voltage, output current and inductor current respectively. It is observed that the mean of the output current is 10A which is expected. However, the output current ripple is 3 $A_{p-p}$ which is above the allowed ripple.

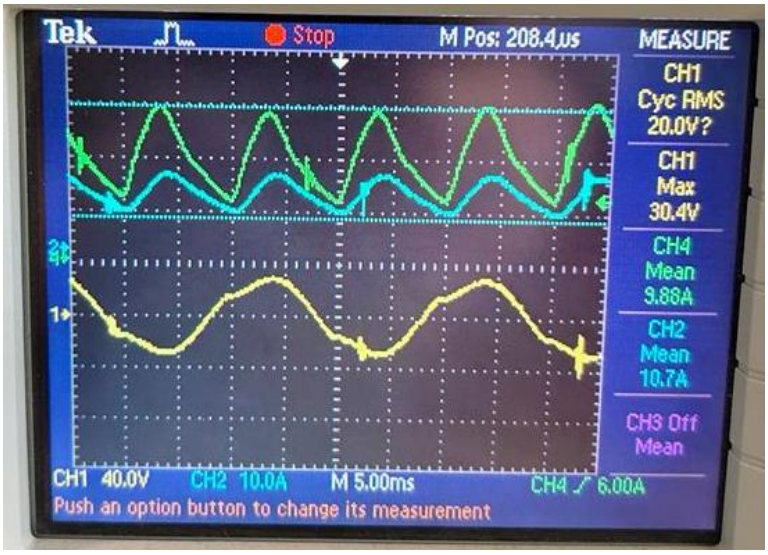


**Figure 23. Test Results with R Load 10A**

## Demo Day Test Results

In the demo the circuit is connected to the battery and the charging current is set to 10A. The connections are given in Figure 24. At first 13 $V_{rms}$ is applied to rectifiers input. The input side measurements are given in Figure 25. The battery voltage is measured as 13.4V while charging. Oscilloscope readings for output current (CH4) and inverted drain source voltage (CH3) are given in Figure 14. The average output current is approximately 10 A, and the ripple is approximately 2A which are expected. Moreover, one can observe the switching from the drain to source voltage. The duty cycle is measured as 0.67. The analytical duty cycle can be calculated as follows.

$$D = \frac{I_{in}}{I_{out}} = \frac{7.65}{10} = 0.765$$

$$D = \frac{V_{out}}{V_{in}} = \frac{13.2}{(1.35)\,(13)} = 0.764$$

The discrepancy between the measurements and the analytical results occurs due to the losses of the components and the power consumed on the fans, Arduino UNO, and gate driver. Let's calculate the efficiency of the charging circuit.

$$efficiency = \frac{P_{out}}{P_{in}} = \frac{(9.4)\,(13.2)}{161.25} = 0.768 = 76.8\%$$

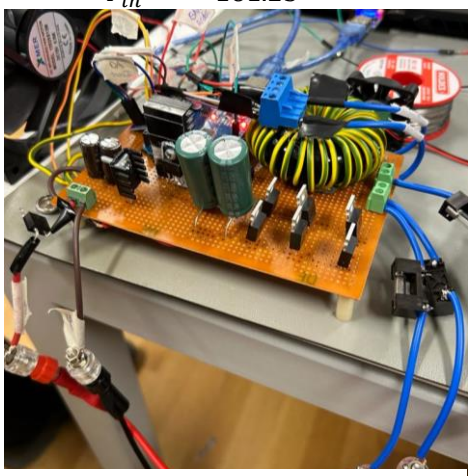

**Figure 24. Demo Setup**

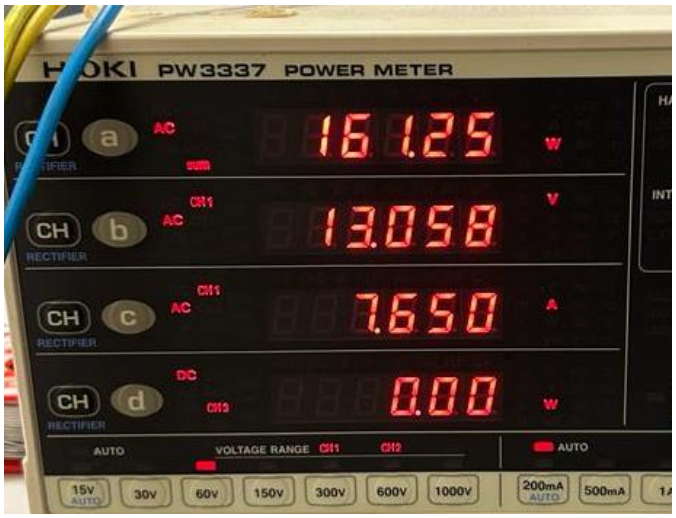


**Figure 25. Input Side Measurements**


**Figure 26. Output Current and Vds for 13Vrms Input**

Then input voltage is increased to 20 $V_{rms}$ and it is observed whether the output current is regulated to 10A. The oscilloscope readings are given in Figure 15. CH1 and CH3 measure the input voltage and drain to source voltage respectively. CH2 and CH4 measure the output and inductor current respectively. Since input voltage is increased to keep output current same the duty cycle is decreased. This can be observed in CH3. Also, the mean output current is 9.38A. However, this time the output current ripple condition is not satisfied. The current ripple is approximately 5A.


**Figure 27. Oscilloscope Measurements for 20Vrms**

In demo session thermal concerns are the number one problem. The temperature of the rectifier diodes, MOSFET and the buck converter diode must be kept below $170\ °C$. The image taken from the thermal camera after 5 minutes of charging is given in Figure 28. From Figure 28, it can be seen that buck converter's diode reaches the maximum temperature which is $62\ °C$ well below the rated value.

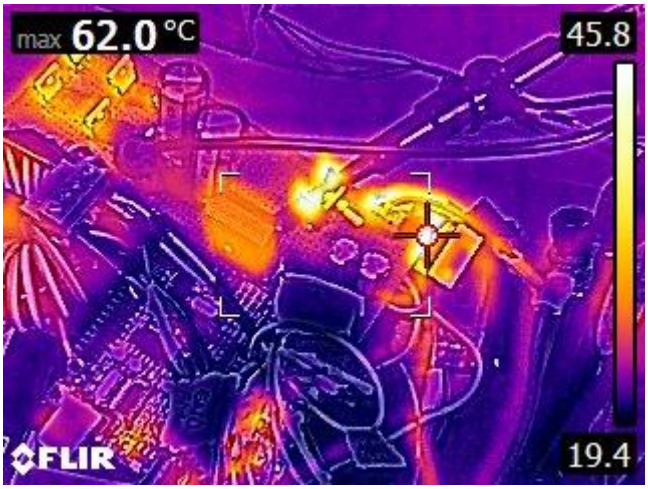


**Figure 28. Thermal Results After 5 Minutes of Battery Charging**

# Physical Properties

## Thermal Analysis

Thermal design holds a very crucial role in power electronics design due to the temperature vulnerable components. Otherwise, components may be harmed due to overheating. The reason behind the increase in the temperature is power losses. Hence, we will start by making power loss calculations.

The main power losses that are detrimental in terms of heating occur on the semiconductors. Hence the following semiconductors are investigated in terms of heating due to switching and conduction losses.

- Rectifier Diode DSS16-01A
- Buck converter diode DSA30I100PA
- Buck converter MOSFET IRF540N

The switching and conduction losses are calculated for the worst case and the ambient temperature is assumed to be 25 °C during the calculations.

- **Rectifier Diode DSS16-01A**

DSS16-01A is a Schottky diode hence its reverse recovery time is 0. Also, in the datasheet it is indicated that the switching losses are negligible compared to conduction losses. Hence, only conduction losses are considered for rectifier diode.

$$P_{conduction} = I_{F,rms} V_F$$

The maximum rms forward current occurs when input voltage is 15 $V_{rms}$ and it is measured from the simulation environment as 3.377 $A_{rms}$. The forward voltage drop on the diode is 0.64 V which is available in the datasheet.

$$P_{conduction} = (3.377)(0.83) = 2.16\,W$$

The thermal lumped parameter circuit of this diode without a heatsink is given in Figure 29.

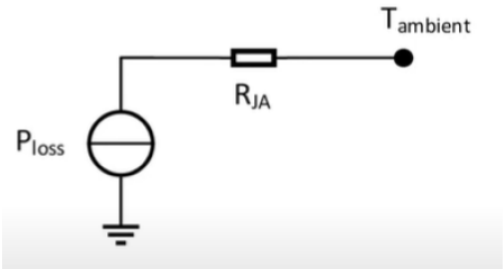


**Figure 29. Thermal Lumped Parameter Circuit Without Heatsink**

The junction to ambient resistance is given as 44.6 °C/W in the datasheet.

$$(T_{junction} - T_{ambient}) = P_{loss}\, R_{JA}$$

$$T_{junction} = T_{ambient} + P_{loss}\, R_{JA} = 121\,°C$$

- **Buck Converter Diode DSA30I100PA**

This diode is also a Schottky diode and in datasheet it is indicated that switching losses are negligible compared to conduction losses. From the datasheet the forward voltage is indicated as 0.78 V. The rms forward current is measured from the simulation as 7.64 $A_{rms}$.

$$P_{conduction} = I_{F,rms} V_F = (7.64)(0.78) = 5.96\,W$$

The typical thermal resistance of junction to case and case to heatsink are provided as 0.85 °C/W and 0.5 °C/W in the datasheet. 578622B03200G heatsink compatible with TO220 packaging is selected. Thermal resistance of this heatsink is 13.2 $°C$/W. The thermal circuit with heatsink is given in Figure 30.

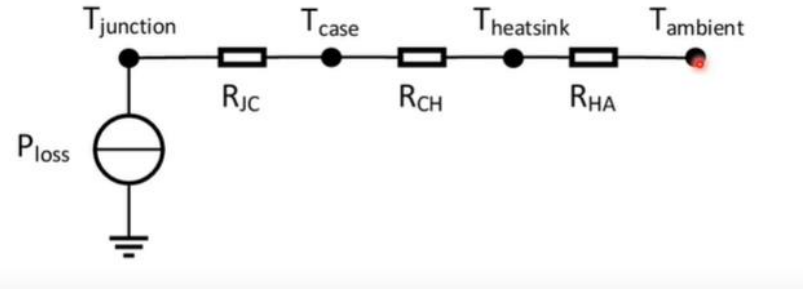


**Figure 30. Thermal Lumped Parameter Circuit with Heatsink**

$$(T_{junction} - T_{ambient}) = P_{loss}\,(R_{JC} + R_{CH} + R_{HA})$$

$$T_{junction} = T_{ambient} + P_{loss}\ (R_{JC} + R_{CH} + R_{HA}) = 106.2\,°C$$

The maximum allowed junction temperature is 175 °C according to the datasheet.

- **Buck Converter MOSFET IRF540N**

The RMS of the current flowing on the MOSFET is 6.56 A according to the simulations. Drain to source voltage is indicated as 0.04 Ω in the datasheet. Hence conduction losses can be calculated as follows.

$$P_{conduction} = {I_{F,rms}}^2 R_{ds} = 1.24\,W$$

The switching losses can be calculated from the below formula.

$$P_{sw(ON)} = \frac{1}{6}(V_{ds} \cdot I_d) \cdot t_r \cdot f_{sw}$$

$$P_{sw(OFF)} = \frac{1}{6}(V_{ds} \cdot I_d) \cdot t_f \cdot f_{sw}$$

$$P_{sw} = P_{sw(ON)} + P_{sw(OFF)}$$

According to the simulation results

$$P_{sw(ON)} = (33.14 \cdot 15.73) \cdot 57 \cdot 10^{-9} \cdot 50 \cdot 10^{3} = 1.486\,W$$

$$P_{sw(OFF)} = (34.03 \cdot 28.61) \cdot 55 \cdot 10^{-9} \cdot 50 \cdot 10^{3} = 2.7W$$

$$P_{sw} = 4.184W$$

$$P = P_{sw} + P_{conduction} = 5.42\,W$$

As heatsink the heatsink used in 150W DC-DC Boost Converter's heatsink which is given in Figure 31 is used. Since the datasheet cannot be found the thermal resistance will be accepted as 16 °$C$/W. The thermal resistance of junction to case is 1.25 °$C$/W and the thermal resistance of the thermal paste is assumed to be 0.5 °$C$/W.

$$(T_{junction} - T_{ambient}) = P_{loss}\,(R_{JC} + R_{CH} + R_{HA})$$

$$T_{junction} = T_{ambient} + P_{loss}\ (R_{JC} + R_{CH} + R_{HA}) = 121.2\,°C$$

The maximum temperature the MOSFET's junction can withstand is 175 °C.

**Figure 31. 150W DC-DC Boost Converter**

Since the diode and MOSFET's temperature are a little close to the maximum rated temperature a 92x92x25mm 3000rpm fan is used. The fan and the cooling setup are given in Figures 32 and 33 respectively.

**Figure 32. 92x92x25mm 3000rpm Fan**

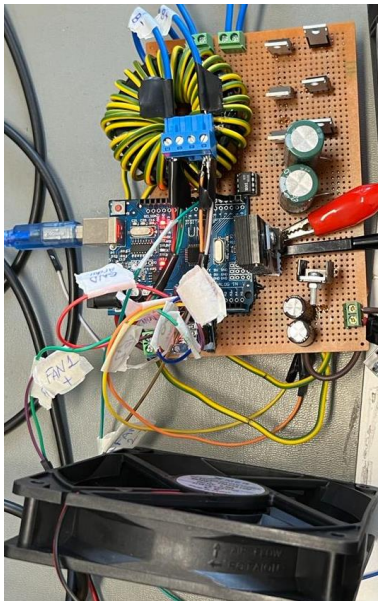

**Figure 33. Cooling Setup**

By cooling the circuit, the thermal resistance of the heatsinks can be lowered up to 4 °C/W.

## Size Analysis

The board that the circuit is built on is measured from its longest edges and the total volume is calculated accordingly. The measurements are given below:

$$Length = 15cm$$

$$Width = 10cm$$

$$Height = 9cm$$

$$Total\ Volume = 15cm \cdot 10cm \cdot 9cm = 1350cm^3 = 0.00135m^3$$

## Cost Analysis

For the cost analysis, the prices given in the Table 5 are calculated as follows:

$$Total\ Price = Quantity\ of\ the\ Component\ in\ 1\ Circuit \cdot 1000$$

Also, for the PCB production, the cost of producing 1000 2 layered PCBs are calculated using tools of PCBWay.

**Table 5. Cost Analysis of the Product for 1000 Pieces**

| Component | Total Price ($) |
|---|---|
| IRF540N | 838.29 |
| IR2106 | 730.38 |
| DSS16-01A | 4630.20 |
| DS30I100PA | 1038.96 |
| WL1V477M10020PA | 249.36 |
| PKLH-063V102MJ355 | 757.80 |
| 0079192A7 Core | 7971.31 |
| ACS712ELC-30A | 1046.36 |
| LM2596 DC-DC Step Down Converter | 840.54 |
| Arduino UNO | 5968.42 |
| Fan | 3088.37 |
| PCB | 1319.60 |

$$Total\ Cost = 28.480k\$\ for\ 1000\ Pieces$$

$$1\ Product = 28.48\$$$

# Conclusion

This report examines the process of design, implementation, and testing processes of the Wind Turbine Battery Charger project. In the design step, considering the final requirements of the project, topology research has been done, and the team decided on building a three-phase diode rectifier with a buck converter. The research and simulation part helped the team to understand the topologies and find solutions to the predetermined or possible errors. Then, the implementation step started, which was the most educatory part of the project. During the production of the circuit, and connecting different modules with each other, tons of unexpected problematic situations have occurred. The members have gained tons of experience while solving these problems and understood the difference between a simulation environment and a real-life application. Lastly, the circuit was presented on the "Demo Day". The results of the successfully implemented battery charging process and other testing processes are given.

# References


[1] (PDF) Practical design of Buck Converter by Taufik - Researchgate. (n.d.). https://www.researchgate.net/publication/321903540_Practical_Design_of_Buck_Converter_By_Taufik

[2] Basic calculation of a Buck Converter's power stage. (n.d.). https://www.ti.com/lit/an/slva477b/slva477b.pdf

[3] Wikimedia Foundation. (2023, February 27). Internal resistance. Wikipedia. https://en.wikipedia.org/wiki/Internal_resistance#:~:text=A%20battery%20may%20be%20modeled,involving%20concentrations%20and%20reaction%20rates.

[4] Tracer 12V 100ah lifepo4 battery module. Tracer Power. (2023, September 28). https://tracerpower.com/products/batteries/tracer-12v-100ah-lifepo4-battery-module/

[5] K. Mμ *et al.*, "POWDER CORES." Accessed: Jan. 23, 2024. [Online]. Available: https://www.mag-inc.com/Media/Magnetics/File-Library/Product%20Literature/Powder%20Core%20Literature/Magnetics-Powder-Core-Catalog-2020.pdf